2007-5129

43rd AIAA/ASME/SAE/ASEE Joint Propulsion Conference, 9-11 July 2007, Cincinnati, Ohio

Radiofrequency Plasma Thrusters: Modelling of Ion Cyclotron Resonance Heating and System Performance

Vito Lancellotti, Giuseppe Vecchi, Riccardo Maggiora,

Politecnico di Torino, Dipartimento di Elettronica, Torino, I-10129 Italy

Daniele Pavarin, Simone Rocca,

CISAS G. Colombo, Padua University, Padova, I-35131 Italy

Cristina Bramanti,

Advanced Concepts Team, ESA-ESTEC, Noordwijk, The Netherlands

Recent advances in plasma-based propulsion systems have led to the development of electromagnetic (RF) generation and acceleration systems, capable of providing highly controllable and wide-ranging exhaust velocities, and potentially enabling a wide range of missions from KWs to MWs levels. In this paper we report on the development of a system-level modelling of a three-stage helicon plasma thruster composed of a helicon plasma source, a confining magnetic field structure enclosing a plasma heating section, and a magnetic nozzle. This modelling can help to optimize the design parameters (antenna shape, matching circuits and generators, and the ensuing evaluation of the required power, mass and other physical parameters, including magnetic field for confinement), and estimate the system feasibility: in particular our activity focuses on the most critical RF issues and on the RF-plasma interactions. We have divided the study into two different and linked parts: 1) RF system modelling, which provides an "interface" between the RF power generation and the power deposition into the plasma and relies on the TOPICA code, and 2) plasma device modelling of the sub-systems and of their connection, which yields the global, system-level description of the engine.

I. Background and motivations

Plasma-based propulsion systems have found increasing interest in the past twenty years. Their conception and design derives directly from magnetic confinement fusion research, particularly of open magnetic "mirror" devices. Recent advances in plasma-based concepts have led to the identification of electromagnetic (RF) generation and acceleration systems as able to provide not only continuous thrust, but also highly controllable and wide-ranging exhaust velocities. This is of particular advantage in maneuvering applications such as planetary missions involving planetary orbit insertion/transfer and deep space cruise phases. Another key feature of RF based plasma systems is their ability to produce energetic exhaust flows starting from light gases (H_2, D_2, He) giving very high specific impulse (up to 30,000 s) to heavier noble gases (Ar, Kr, Xe) with lower specific impulse but higher thrust; a side benefit of these RF-based designs is that they are electrode-less, with the related long device lifetimes since sputtering problems due to ion impingement on grids is avoided. Furthermore, they are scalable from low-power (few kW) to high-power (¿100 kW), thus making them suitable for a variety of mission applications. In particular, for missions in the 100 kW-MW class, the constraint of present electric propulsion system (gridded ion, Hall Effect) lead to the necessity of large modules integrating a cluster of thrusters with a high number of power processing units, and therefore high propulsion system masses and volumes. Alternative propulsion technologies with higher power and thrust densities and moderate/high specific impulse, such as RF plasma thrusters, could provide high advantages in terms of mass and volumes savings.

It is also to be stressed that these plasma thrusters have terrestrial applications in other sectors such as surface science, high-energy physics, and waste disposal.

The typical conceptual design of an RF plasma thruster is composed of an RF plasma source, an open-ended magnetic confinement device, an RF acceleration unit, and a "magnetic nozzle" (that might not be distinct from the confinement device). The plasma source is composed of an RF driven helix-like antenna ("helicon") that energizes a flow of initially neutral gas, into magnetised plasma with high ionization fraction. The plasma outflow is confined into an elongated column by an intense magnetic field system, and then accelerated by a second RF driven device before exhaust flux through the "magnetic nozzle" structure of the magnetic field produced by the confinement coils near the acceleration region. The plasma source and the acceleration unit employ distinct RF systems and frequencies; the ubiquitous choice for the acceleration is to employ the Ion-Cyclotron Resonance Frequency (ICRF), a proven technology in fusion experiments for efficiently transferring large RF powers to magnetized plasmas, and exploited by the NASA VASIMR (VAriable Specific Impulse Magnetoplasmadynamic Rocket) propulsion system.[1,2] However, despite their distinct advantages in terms of performance of other forms of electric propulsion, some major challenges need to be overcome. These are primarily related to reducing the presently high specific mass and the large geometry of the system, as well as improving the thrust efficiency (at present the specific power is very high).

In present paper we report on the development of a system-level modeling of a three-stage plasma thruster composed of a helicon plasma source, a confining magnetic field structure enclosing a plasma heating section, and terminating into a magnetic nozzle. This modeling can be employed to optimize the design parameters (antenna shape, matching circuits and generators, and the ensuing evaluation of the required power, mass and other physical parameters, including magnetic field for confinement), and to estimate its feasibility: in particular our activity focuses on the most critical RF issues and on the RF-plasma interactions. The modelling has been divided into two different and linked parts: RF system modelling and modelling of the plasma device. The RF systems modelling activity provides an "interface" between the RF power generation and the power deposition into the plasma. The plasma modelling of the sub-systems and of their connection provides the global, system-level model of the engine. The usual choice for the thruster acceleration unit is to employ the Ion-Cyclotron resonance frequency (ICRF), a well established technology in fusion experiments for transferring large RF powers to magnetized plasmas. To help design RF thruster ICRF antennas, TOPICA (Torino Polytechnic Ion Cyclotron Antenna) code has been recently extended to handle cylindrically symmetric plasmas (Fig. 1b).

The latter entailed developing a wholly new module of TOPICA charged with the task of solving Maxwell's equations in cylindrical magnetized warm plasmas and yielding the Green's function $\breve{\Upsilon}(m, k_z)$, i.e. the relationship at the air-plasma interface between the transverse magnetic and electric fields in the spectral (Fourier) domain. The approach to the problem of determining the antenna input impedance relies on an integral-equation formulation for the self-consistent evaluation of the current distribution on the conductors. The simulations are aimed at improving the penetration and coupling of the ICRF waves with the magnetized plasma in order to enhance plasma heating and axial thrust. An electromagnetic model of the plasma device has been developed in order to provide an appreciation of its performance. As previously mentioned, the model describes the three stages of the device: plasma generation, plasma heating and plasma detachment. In the plasma generation section each species is followed in the electron impact reactions of ionization, dissociation, recombination, and excitation. In the heating stage the plasma absorbs the power emitted by the antenna ICRF, and in the magnetic nozzle the thermal energy of the plasma is converted into kinetic energy and the plasma is exhausted. This tool makes it possible to evaluate the required power, mass and other physical parameters, including magnetic field for confinement. In particular, the feasibility of a low-power (a few kW) system will be presented, and the scaling to high power addressed. The resources required for its physical realization will be finally estimated in terms of power, dimensions, mass etc. Finally, critical technologies will be defined and necessary development steps outlined.

II. Antenna problem formulation

The main purpose is to determine the admittance matrix $[Y]$ of an arbitrarily shaped antenna operating within the ICRF acceleration unit of a plasma thruster. If the antenna is feeded by N_P coaxial lines, then N_P is the total number of feeding ports and $[Y]$ comes to be an N_P-order matrix: in Fig. 1 a cross-sectional view of the structure under study is schematically depicted. A widely-used configuration of the RF booster comprises two counter-driven loops antennas encircling the plasma column (see Fig. 1), but we

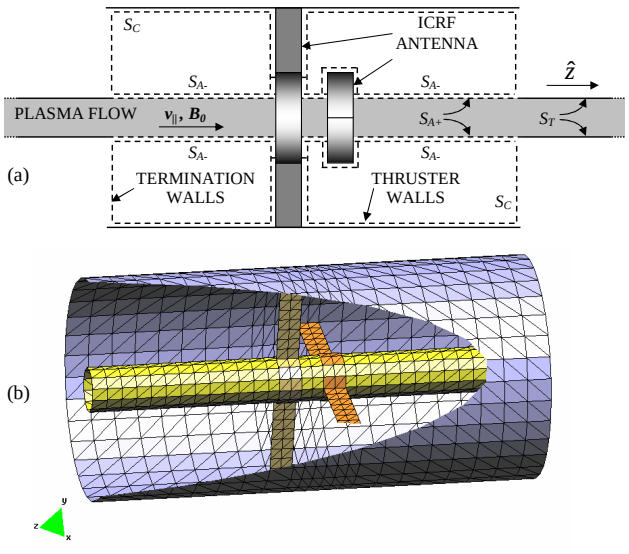

Figure 1. ICRF unit model of a typical RF thruster featuring two loop antennas and plasma flow: (a) cartoon with the surfaces whereon the EP is applied and (b) clipped for visualization's sake, a CAD model showing the 3D surface triangular-facet mesh for simulations with TOPICA; in that regard, S_T needs neither be defined nor meshed, as the plasma Green's function allows for its effect.

want to emphasize that the approach developed allows considering any shape of the antenna—and of the acceleration unit. By contrast we require the magnetically confined plasma to exhibit a circular cross section.

Owing to the underlying formulation[3] of the EM problem, the plasma enters the equations only via its pertinent dyadic Green's function $\tilde{\Upsilon}(m, k_z)$ in the Fourier space, i.e. the rank-2 tensor linking the transverse-to-$\hat{\rho}$ magnetic and electric fields at the air-plasma interface ($\rho = a$):

$$-\tilde{\mathbf{H}}_t(a; m, k_z) \times \hat{\boldsymbol{\rho}} = \tilde{\Upsilon}(m, k_z) \cdot \tilde{\mathbf{E}}_t(a; m, k_z), \qquad \tilde{\Upsilon} = \begin{bmatrix} \boldsymbol{Y}_{\theta,\theta} & \boldsymbol{Y}_{\theta,z} \\ \boldsymbol{Y}_{z,\theta} & \boldsymbol{Y}_{z,z} \end{bmatrix}, \tag{1}$$

with m (k_z) being the azimuthal (longitudinal) wavenumber. Therefore, a brand new module has been developed in charge of solving Maxwell's equations within a magnetized cylindrically-symmetric radially-inhomogeneous warm plasma and then yielding $\tilde{\Upsilon}(m, k_z)$. As per the plasma model, the high speed plasma flow, occurring in the RF thrusters, is assumed to rapidly and wholly absorb the ion cyclotron waves launched by the antennas;[4] besides, the plasma velocity, whose main effect is to shift the ion cyclotron frequency,[5] is accounted for as well. Finally, no limitations at all are posed to the antenna shape, hence the present version of TOPICA represents a substantive improvement of a previous simplified approach.[6]

According to Fig. 1a, our thruster model assumes the plasma faces the antennas—and all the other conducting bodies, for that matter—only through a cylindrical surface S_{A+} (dubbed *aperture*) of finite extent, which is cut out off an otherwise infinite metallic cylinder coaxial to the plasma itself. As can be seen in Fig. 1b, the fictitious walls and the aperture constitute a *cavity*—vaguely reminiscent of a drum with a median hole—wherein the antennas exist and work. The validity of our ICRF stage model can be backed as follows: for one thing, the whole structure size is usually several order in magnitude smaller than the vacuum wavelength, in view of the very low operating frequency (about 1 MHz is common), then we have the distance (h) between the cavity's top and bottom walls large enough as compared to the antenna size. Under those circumstances, we do expect h and the fictitious boundaries not to affect the antenna parameters significantly, although their sensitivity to h can be easily studied.

Now, the electromagnetic problem shown in Fig. 1a is formulated exactly the same way as in[3] in terms of two coupled integral equations, which entails invoking the Equivalence Principle (EP)[7] twice and then enforcing the boundary and continuity conditions the tangential fields obey on S_C, $S_{A\pm}$. This two-step application of the EP yields two unknown surface current densities, $\mathbf{J}_C$ and $\mathbf{M}_{A-}$; the fields dependence on $\mathbf{J}_C$, $\mathbf{M}_{A-}$ is linear and represented by surface integrals with appropriate kernels (i.e. Green's functions).[8] Specifically, inside the cavity we use the free space scalar Green's function, whereas on the plasma side (S_{A+}) we need employ $\tilde{\Upsilon}$ defined in (1). The integral equations are solved by the Moment Method,[9] both

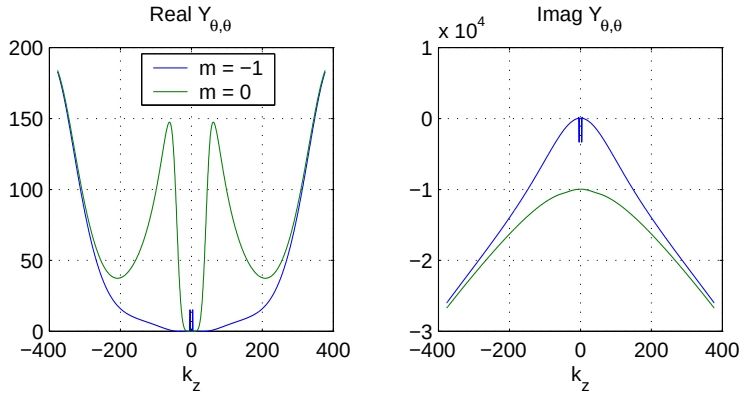

Figure 2. Plasma Green's function entry $\tilde{Y}_{\theta,\theta}/Y_0$ for the azimuthal wavenumbers m = -1, 0, as a function of the longitudinal wavenumber k_z/k_0, with Y_0 (k_0) being the free space admittance (wavenumber).

Table 1. Geometrical and physical data, single species ($^4He^+$) plasma

Height (m)	0.4	Density at center (m^{-3})	5.55 10^{19}
Loop radius (m)	0.021	Density at edge (m^{-3})	0
Loop width (m)	0.02	Axial magnetic field (T)	0.2
Loop distance (m)	0.02	Parallel velocity (m/s)	8 10^3
Plasma radius (m)	0.02	Ion perp./par. temp. (eV)	1
Frequency (MHz)	0.765	Electron perp./par. temp. (eV)	4.7

in spatial and spectral domain, the latter being the one wherein the plasma is more easily described. To be concrete, $\mathbf{J}_C$, $\mathbf{M}_{A-}$ are expanded as a linear combination of a finite set of subdomain basis functions, which are defined over triangles (see Fig. 1b). The coefficients of these linear combinations represent the actual unknowns of the problem, which is turned from a set of integral equations into an algebraic system.

III. Preliminary antenna results

The formulation outlined above has been implemented in TOPICA, so that, once the current densities $\mathbf{J}_C$, $\mathbf{M}_{A-}$ have been computed, the antenna admittance matrix $[Y]$ along with other common parameters[3] can be obtained. The code has been thoroughly tested in vacuum, while preliminary results with plasma show good agreement with data available in literature.

To give an example of TOPICA's capabilities, we consider a neutral electron-helium ($^4He^+$) plasma and a two-loop ICRF antenna as in Fig. 1b: listed in Table 1 are the main parameters used for the simulation. The density profile has been assumed parabolic and given analytically, though it may be read from file if desired.

An important intermediate step towards the solution is the calculation of the Green's function $\tilde{\mathbf{Y}}(m, k_z)$, which accounts for all the plasma effects. Extensive numerical experiments have shown that, in the light of the average size of the triangular facets forming the aperture mesh (see Fig. 1b), it suffices to determine $\tilde{\mathbf{Y}}(m, k_z)$ for m running from -60 to 60 (i.e. a total of 121 azimuthal modes), in order for the spectral integrals to converge.[3] For sake of completeness, drawn in Fig. 2 are the first two modes of $Y_{\theta,\theta}$ germane to the case under study.

In our investigations, we considered a standard counter-driven two-loop antenna, as in Figs. 3 and Fig. 4, but also experimented new antenna shapes. In that regard, we tried, among others, electrodes constituted by two disjoint half-loops, as can be seen in Figs. 5 and 6 below, which as a whole we dubbed a capacitor antenna. Also shown in Figs. 3 through 6 are the electric (magnetic) surface current densities over the conducting bodies (at the air-plasma interface), when the antenna terminals are driven by $\{+V, -V, +jV, -jV,\}$, respectively, since we want the complete antenna to launch an electric field with the circular polarization that maximizes the wave coupling to the $m = -1$ mode.[2] As expected the electric current is almost a constant over the antenna loops, in the standard configuration, owing to the large vacuum wavelength as

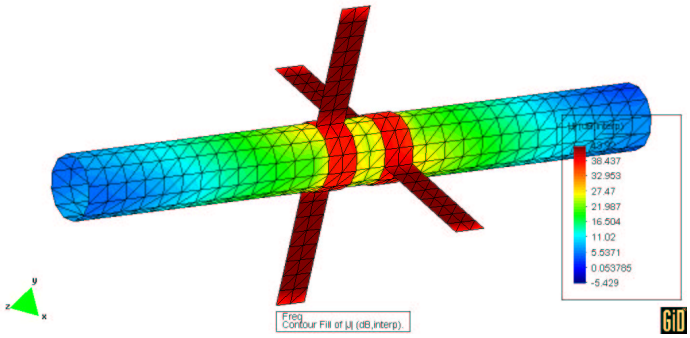

Figure 3. Standard counter-driven two-loop antenna: sample electric current magnitude distribution on conducting bodies and at plasma/air interface.

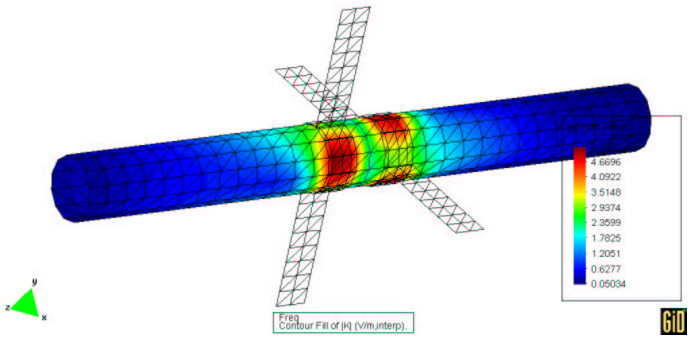

Figure 4. Standard counter-driven two-loop antenna: sample magnetic current magnitude distribution at plasma/air interface.

compared to overall structure size. Besides, the magnetic current magnitude (that's to say the tangential electric field) is quite strong under the loops, which agrees with the expectation.

The main TOPICA's output is the antenna 4-by-4 admittance matrix $[Y]$, which in this instance may be further reduced to a 2-by-2 matrix, for each loop is counter-driven with voltages. Upon knowing $[Y]$, one can compute the total power P_{rad} absorbed by the system and hence the coupling resistance—a key figure of merit that characterizes the ICRF antennas efficiency for thruster applications—as $R_c = 2P_{\text{rad}}/|I|^2$, wherein I identifies the current entering the antenna terminals. As an example, assuming $V = 1$ V, we computed the absorbed power and the loading R_c for the two cases (standard and non-standard) and found that the coupling resistance attained with the new electrodes can be about 20% higher than the typical values featured by the two-loop antenna. This result is itself pretty amazing but also suggestive of the powerful capabilities of TOPICA as a numerical tool to help design and optimize the ICRF antennas.

As for the technological issues involved in the overall system design, we point out that the thermal aspects need to be assessed as well and an adequate thermal control system incorporated as necessary, which is due to the high power required to supply an increased plasma density in the ICRH. Finally, superconductive magnets should then be used in order to allow a more compact and less complex system, with respect to conventional magnets. The next step for a future development would be to implement the results obtained by TOPICA, in order to optimize the RF design and the thruster design at different power levels and to arrive to a detailed system design.

IV. Plasma thruster modelling

A numerical model that describes the physics of the thruster is useful for a number of reasons: it permits to understand the physics of the mechanisms involved, it gives direction on the optimization and design of the experiment, it permits to predict the performance of the thruster, and it contributes to reduce the number of experiments required. The model resembles the three physical stages of the thruster: the plasma

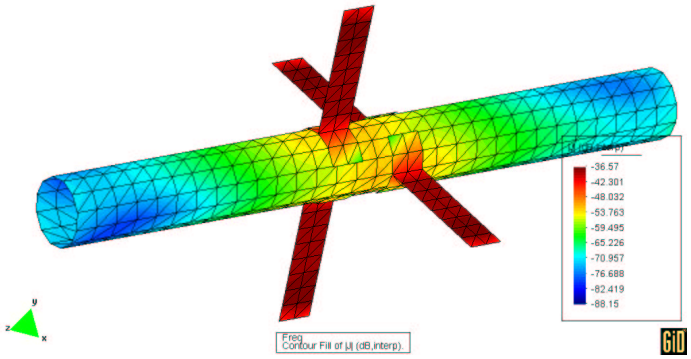

Figure 5. Capacitor antenna: sample electric current magnitude distribution on conducting bodies and at plasma/air interface.

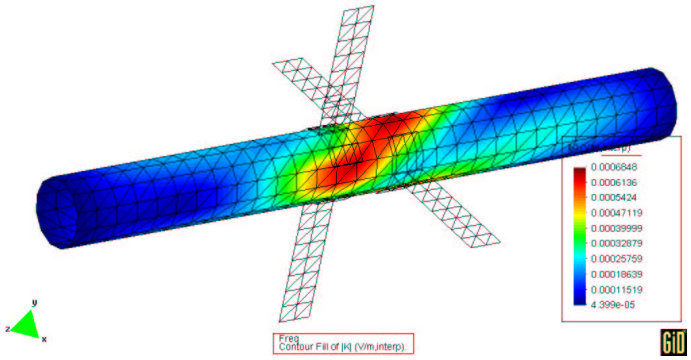

Figure 6. Capacitor antenna: sample magnetic current magnitude distribution at plasma/air interface.

discharge, the RF plasma acceleration, and the magnetic nozzle. Aim of this section is to provide a global time dependent model of a helicon source developed for producing plasma density above 10^{18} m$^{-}3$. The model combines a global plasma source simulation with a 0-dimensional gas-dynamic simulation. It accounts for changes in the neutral density, ionization, excitation and dissociation. Outputs of the model are: the density of each neutral and ionized specie, the electron density and temperature and the time history of each particle/energy loss channel.[10–12]

IV.A. Plasma reactions

The plasma balance equations, for particles and energy, have been written for describing uniformly distributed plasma inside of a region determined by the magnetic field configuration. The neutral interaction with plasma has been considered in this work by coupling a 0-dimensional gas-dynamic model of the entire system, with a global plasma model of the source. The interactions taken into account in the model are:

- neutral density reduction due to ionization;
- neutral dissociation (molecular species-atom species);
- zero dimensional gas dynamic analysis behavior in the plasma source and in the vacuum chamber;
- wall recombination and volume recombination in the main vacuum chamber.

The particle balance equations for the ionized particles and electrons are written in a particle flux form, (particles/seconds m^3). The general form for the balance equations of charged particles is:

$$\frac{dn_i}{dt} = \Gamma_i^s - \Gamma_i^l - \Gamma_{W,i} - \Gamma_{EXH,i} \tag{2}$$

Γ_i^s is for the i-specie the source term due to plasma processes, Γ_i^L is the loss term due to plasma processes, Γ_{Wi} is for the i-specie the loss term due to particle recombination at the wall (the particle diffuses through the

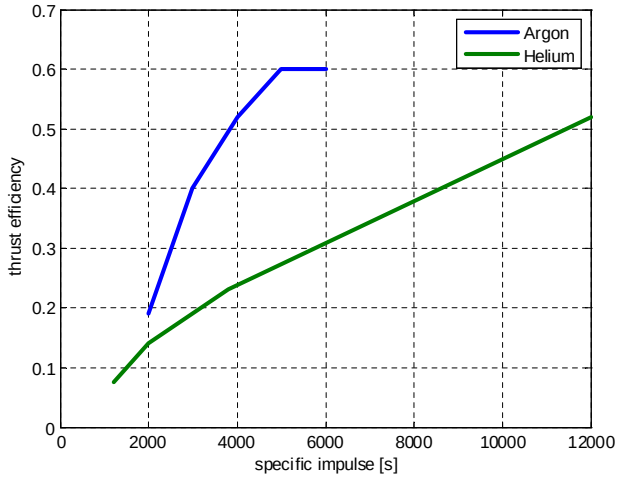

Figure 7. Thrust efficiency as a function of the specific impulse using helium and argon.

wall sheath before reaching the wall), $\Gamma_{EXH,i}$ is the loss term due to the particle flow through the exhaust. The reaction rates were obtained averaging the cross section for the specific reaction over a maxwellian distribution:[14]

$$K_{iz} = \left(\frac{m}{2\pi k T_e}\right)^{3/2} \int_0^\infty \sigma(\nu)\nu \exp\left(-\frac{m\nu^2}{2kT}\right) 4\pi\nu^2 d\nu \tag{3}$$

where T_e is the electron temperature in eV and m is the electron mass and σ the cross section. Wall losses are calculated as in.[10–12] Ions lost at the exhaust are calculated as:

$$L_{EXH} = n_i u_B A_{EXH} \tag{4}$$

$$u_B = \sqrt{kT_e/m_i} \tag{5}$$

with u_B the ion Bohm's velocity and A_{EXH} is the geometrical exhaust area.

Another parameter affects the exhaust flow. At the exit of the plasma discharge section the magnetic field increases and then decreases. This peak acts as a magnetic mirror that reflects part of the plasma flow. Therefore the net flow is given by the difference between the incident flow and the reflected flow. To calculate the electron temperature, the power balance equation has been written as follows (units W/m^3):

$$\frac{P_{ABS}}{V_e} = \frac{d}{dt}\left(\frac{3}{2} e n_e T_e\right) + \sum_i P_i + P_W + P_{EXH}, \tag{6}$$

P_{ABS} is the deposited power into the plasma, which is assumed to be known, e is the electron charge, T_e is the electron temperature, V_e again the plasma volume, the P_i terms are the power lost in the i-reaction. The general formula is:

$$P_i = K_i E_{TH,i} n_e n_j \tag{7}$$

where K_i is the rate constant for the specific reaction, E_{TH-i} the threshold energy for the i-reaction,[15] n_e the electron density, n_j the density of the species involved in the i-reaction, P_W is the power lost at the wall due to the electron-ions flow, P_{EXH} is the power loss associated with the electron and the ion flux at the exhaust, assuming that the escaping velocity is the ion-Bohm velocity. Experimental results[13] indicate the presence of a hot tail in the electron population in hydrogen and helium discharge. This distribution has been modelled summing two maxwellian distributions: one with the temperature of the bulk of the plasma and one with the temperature of the hot tail.

IV.B. ICRH effect

The ICRH is expected to heat the plasma to ion temperatures in the order of 100 eV. Since the helicon heats the plasma to an ion temperatures of less than 1 eV, it seems reasonable to consider cold (T_i=0 eV)

the plasma arriving at the ICRH. Therefore, it has been assumed that the plasma flow entering the ICRH region is monoenergetic with an axial velocity equal to u_2.

The power deposited by the ICRH is absorbed by the plasma in the form of normal kinetic energy:

$$\frac{1}{2}mv_{\perp 2}^2 = \frac{P_{ABS}}{n_2 u_2 A_2}. \tag{8}$$

IV.C. Magnetic nozzle

Downstream the ICRH, the magnetic nozzle converts part of the normal kinetic energy of the plasma into parallel kinetic energy, and thus produces thrust. This conversion is effective until the plasma detaches from the magnetic field lines. We assume that the detachment happens when the parallel kinetic energy density ($mnv_{||}^2/2$) becomes greater than the magnetic energy density ($B^2/2\mu_0$).

V. Plasma modelling results

The results of the model can be summarized in Fig. 7 which shows the thrust performance of a 10 kW thruster obtained from the optimization by using the evolutionary algorithms. Analogous simulations made for input powers ranging from 1 kW to 100 kW gave results very similar to those shown. This means that the thruster's efficiency seems not to depend on the input power. The thrust performance increases with the specific impulse basically because less power is needed to ionize the plasma and hence more power is diverted on the ICRH antenna that boosts the plasma.

Although the lumped numerical model developed is simple, it gives a complete description of the physics of the thruster. This makes it possible to simulate the plasma behavior in the desired configuration and to determine the efficiency and thrust performance. The use of a finite-element model would have given more detailed and accurate results, but it would have required longer computational times, not compatible with the optimization process. The results of the model give the indication of the values of plasma parameters that should be expected during the experiment, and thus they give the requirements of the diagnostics needed. In particular the diagnostics should be able to measure plasma densities from 10^{17} m^{-3} to 10^{20} m^{-3} and electron temperatures up to 20 eV. The time evolution shows that the plasma probes should have a frequency pass-band from 0 to 1 kHz.

Acknowledgements

The authors are indebted to Dr Alessandro Cardinali with ENEA, Frascati (Italy), for his providing the plasma tensor expression—which is a key ingredient for TOPICA to compute the relevant Green's function—and for a number of valuable discussions.

References

[1]J. P. Squire *et al.* 2003 *Fusion Science and Technology* **43** 111
[2]A. V. Ilin *et al.* 2004 *Proc. 42 AIAA*, No. 0151
[3]V. Lancellotti *et al.* 2006 *Nucl. Fusion* **46** S476
[4]E. Bearing, F. Chang-Diaz, J. Squire 2004 *The Radio Science Bulletin*, No. 310
[5]V. Ilin *et al.* 2005 *Proc. 43 AIAA*, No. 0949
[6]G. Vecchi *et al.* 2005 *16 Topical Conf. on RF Power in Plasmas,* AIP Conf. Proc., Vol. 787
[7]A. F. Peterson, S. L. Ray, R. Mittra 1998 *Computational Methods for Electromagnetics* (New York: IEEE Press)
[8]L. B. Felsen, N. Marcuvitz 1973 *Radiation and Scattering of Waves* (Englewood Cliffs: Prentice Hall)
[9]R. Harrington 1993 *Field Computation by Moment Methods* (New York: Oxford)
[10]Suwon C. 1996 *Physics of plasmas* **6**, 359-365.
[11]Zorat R. 2000 *Plasma Sources Sci. Tech.* **9** 161-168
[12]Lee C. 1995 *J. Vac. Sci. Tech. A* **13** (2) .
[13]M. I. Panevsky 2003 *Characterization of the Resonant Electromagnetic Mode in Helicon Discharges*, PhD Thesis, University of Texas at Austin
[14]M. A. Lieberman 1994 *Principles of Plasma Discharges and Material Processing* (New York: Wiley)
[15]R. K. Janev 1987 *Elementary processing hydrogen helium plasmas* (Springer-Verlag)